Cell, Vol. 87, 241–251, October 18, 1996, Copyright ©1996 by Cell Press

The Chaperonin ATPase Cycle: Mechanism of Allosteric Switching and Movements of Substrate-Binding Domains in GroEL

Alan M. Roseman,* Shaoxia Chen,* Helen White,* Kerstin Braig,†‡ and Helen R. Saibil*
*Department of Crystallography
Birkbeck College, University of London
London WC1E 7HX
United Kingdom
†Howard Hughes Medical Institute
Yale University School of Medicine
New Haven, Connecticut 06510

Summary

Chaperonin-assisted protein folding proceeds through cycles of ATP binding and hydrolysis by the large chaperonin GroEL, which undergoes major allosteric rearrangements. Interaction between the two back-to-back seven-membered rings of GroEL plays an important role in regulating binding and release of folding substrates and of the small chaperonin GroES. Using cryo-electron microscopy, we have obtained three-dimensional reconstructions to 30 Å resolution for GroEL and GroEL–GroES complexes in the presence of ADP, ATP, and the nonhydrolyzable ATP analog, AMP-PNP. Nucleotide binding to the equatorial domains of GroEL causes large rotations of the apical domains, containing the GroES and substrate protein–binding sites. We propose a mechanism for allosteric switching and describe conformational changes that may be involved in critical steps of folding for substrates encapsulated by GroES.

Introduction

Protein folding in vivo is mediated by a large and diverse group of protein families known as molecular chaperones. In most cases, their mechanism of action is not well understood, but in the case of the chaperonins GroEL and GroES, there is considerable structural and functional information. GroEL has a cage-like double-ring structure of 14 60 kDa subunits, each of which is divided into three domains (Saibil et al., 1993; Braig et al., 1994; Figure 1). The large equatorial domain forms the central core of the structure, providing the interring and most of the intraring contacts, and also contains the nucleotide binding site, adjacent to the junction with the small intermediate domain (Boisvert et al., 1996). The large apical domain is mobile and disordered (Braig et al., 1995), and it possesses binding sites for nonnative substrates and for GroES (Chen et al., 1994; Fenton et al., 1994). At the junctions between domains, potential sites of hinge rotation are found (Braig et al., 1994; 1995). Cryo-electron microscopy (EM) analysis has revealed large domain movements of GroEL, in which the apical domains rotate upwards to bind GroES, a dome-like heptamer of 10 kDa subunits (Hunt et al., 1996), creating a large enclosed space (Chen et al., 1994). The GroEL–GroES complex thus contains two distinct types of substrate protein–binding sites: the open trans site, on the GroEL ring remote from GroES, and the cis site, enclosed by GroES. Substrates are initially bound in the trans site and can be encapsulated by subsequent binding of GroES to the same ring (Weissman et al., 1995; Mayhew et al., 1996). Essential steps in folding may occur while the substrate resides in the cis complex (Weissman et al., 1995, 1996; Mayhew et al., 1996).

The ATPase cycle of GroEL controls cycles of alternate binding and release of both substrate protein and GroES (Martin et al., 1993; Todd et al., 1994; Weissman et al., 1994; Burston et al., 1995; Hartl, 1996). Kinetic studies have revealed positive cooperativity of ATP binding and hydrolysis within the rings (Gray and Fersht, 1991; Bochkareva et al., 1992; Jackson et al., 1993; Todd et al., 1993) and negative cooperativity between the rings (Bochkareva and Girshovich, 1994; Yifrach and Horovitz, 1994; Burston et al., 1995). EM and biochemical studies show negative cooperativity of substrate and GroES binding; once one ring is occupied, the second one has a much lower affinity for the same ligand (Chen et al., 1994; Todd et al., 1994; Yifrach and Horovitz, 1996).

It is clear from biochemical and kinetic studies that ATP binding and hydrolysis profoundly alter the functional state of GroEL complexes (Goloubinoff et al., 1989; Martin et al., 1991; Jackson et al., 1993). The complexes have high affinity for substrate protein in the absence of nucleotide and in the presence of ADP but low affinity in ATP (Staniforth et al., 1994; Yifrach and Horovitz, 1996). Cycles of ATP turnover lead to cycles of substrate binding and release (Jackson et al., 1993; Todd et al., 1994; Weissman et al., 1994). The negative stain EM images of Langer et al. (1992) showed differences between GroEL and GroEL-ADP. Our initial study by negative stain EM on the conformational changes induced by ATP suggested an inward rotation of subunits (Saibil et al., 1993). Subsequently, cryo-EM of frozen-hydrated GroEL-ATP oligomers showed an opening out of the apical domains and some asymmetry between the two rings (Chen et al., 1994). In contrast, a recent crystallographic study of the ATPγS–bound form of GroEL has revealed only very small conformational changes, despite the clear presence of bound nucleotide in a novel nucleotide-binding pocket (Boisvert et al., 1996).

In this study, we have used cryo-EM and three-dimensional (3-D) reconstruction to map out the domain movements in chaperonin complexes in the presence of nucleotides. The apical domains, particularly in the region of the substrate- and GroES-binding sites, show a large repertoire of hinge rotations and distortions in the different functional states. Changes in the contacts between rings suggest a mechanism of allosteric switching via a direct connection to the ATP binding site.

‡Present address: MRC Laboratory of Molecular Biology, Cambridge CB2 2QH, United Kingdom.

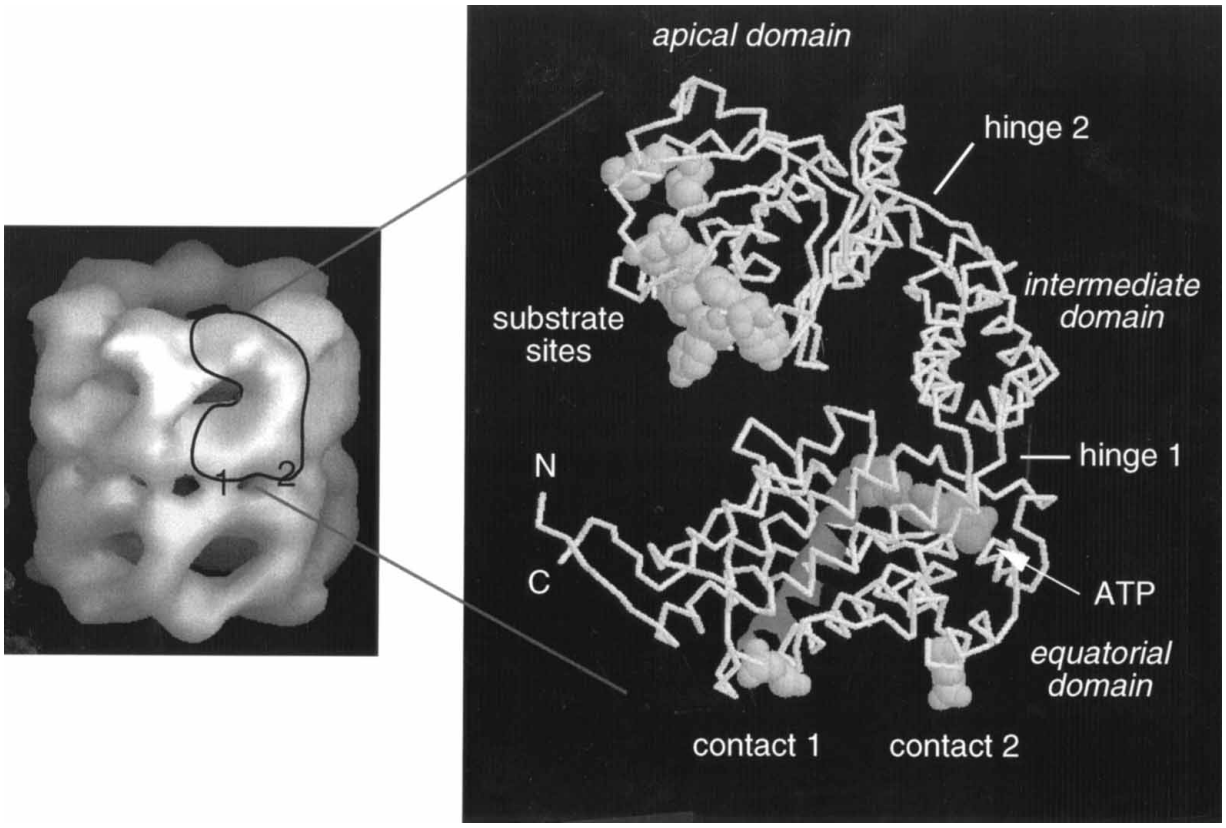

Figure 1. GroEL Structure

Structure of the GroEL 14 mer with one subunit outlined (left) and expanded to show the polypeptide backbone (right) from the X-ray crystallographic results of Braig et al. (1994, 1995). The oligomer structure on the left was produced from the atomic structure, filtered to 25 Å resolution, and shown as a rendered surface. Two bridges of density, numbered 1 and 2, link each subunit to two others on the opposite heptameric ring. Right, each subunit contains three domains: equatorial, intermediate, and apical. The equatorial domain contains the interring contacts and the ATP binding site. A helical segment running between contact 1 and the ATP phosphates is shown as a ribbon. An exposed region of antiparallel polypeptide chains (hinge 1) forms the junction between equatorial and intermediate domains. The small intermediate domain consists mainly of antiparallel α-helices coiled around each other and joins to the apical domain via a second exposed region (hinge 2). The apical domain contains the substrate-binding sites (shown in space-filling form), which coincide with most of the GroES binding sites.

Results

Nucleotides Induce a Range of Conformational Changes in GroEL

Images of frozen-hydrated GroEL complexes (see Figure 2a) show characteristic ring-like end views (along the 7-fold axis) and rectangular side views (perpendicular to the axis). Side views have four layers of density, corresponding to the two stacked rings of subunits, each with two major domains, and end views show the 7-fold symmetry. In the presence of ADP (Figure 2b), the structure is opened out radially (end views) and elongated (side views). Although this is difficult to see on the raw images, it is very obvious once the signal-to-noise ratio is improved by averaging a few views. In the presence of GroES and ADP, bullet-shaped complexes are formed (Figure 2c), and with GroES and AMP-PNP, bullet complexes and some football-shaped (American football) complexes are formed (Figure 2d).

Starting with about 1000 side views of each structure extracted from such untilted images, we have calculated 3-D reconstructions of a set of GroEL–nucleotide complexes by angular refinement against model projections. The structures shown in Figures 3b–3e are reliable to 30 Å resolution. The handedness is not determined by this method and was chosen to match the lower ring (less opened in the nucleotide complexes) to the crystal structure of GroEL (shown as a rendered surface at 30 Å resolution in Figure 3a). The GroEL EM structure (Figure 3b) is in good agreement with the crystal structure to 30 Å resolution, although one cavity is more open than those in the crystal structure (which has exact 2-fold symmetry), and the other is more closed. The crystal structure reveals two interring contacts per subunit (Figure 1); these are not separately resolved at 30 Å.

All of the GroEL–nucleotide complexes show vertical opening and twisting of the apical domains (Figures 3c–3e; ADP, AMP-PNP, and ATP, respectively). Compared with GroEL, the nucleotide-bound structures have all become elongated, and they all show different amounts of apical domain twisting and deviation from 2-fold symmetry. In each case, the ring shown in the upper position is the more open one, and each structure has different apical domain orientations around the cavities. The ADP structure shows the most opening of the rings (Figure 3c). For all the structures, the equatorial

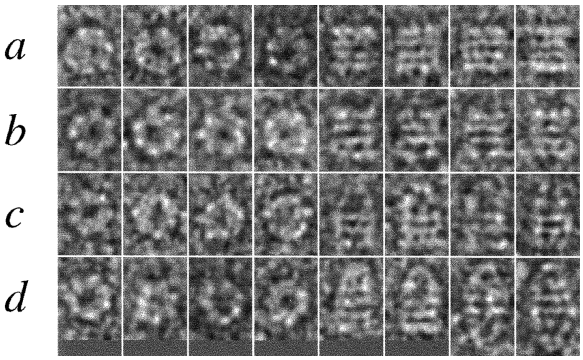

Figure 2. Cryo-EM Images of GroEL Complexes

Cryo-EM images of individual frozen-hydrated GroEL complexes after selection from the original micrographs, alignment, and filtering. A set of four end (round) and four side views (rectangular, with four layers) of each sample are shown.
(a) GroEL,
(b) GroEL-ADP,
(c) GroEL–GroES-ADP,
(d) GroEL–GroES-AMP-PNP. The diameter of the GroEL oligomer is about 140 Å. An increase in separation between the side view layers can be seen in GroEL-ADP (b) relative to GroEL (a). The GroEL–GroES-ADP sample contains bullet-shaped complexes, and the GroEL–GroES-AMP-PNP sample contains bullet and football-shaped (last two views) complexes.

domains are relatively constant, but there are differences in the interring contacts between the ATP structure and all the others. The ATP structure shown was obtained from grids that were vitrified within 4 s of ATP addition; the structure of the steady-state ATP complex appears very similar (data not shown). The ATP structure seems to be a combination of the features previously deduced from negative stain and cryo-EM: the apical domains are vertically extended, but the subunits in the lower ring are rotated inwards. The AMP-PNP structure has an ADP–like upper ring and interring contacts and an ATP–like lower ring.

The domain movements between GroEL and its ADP and ATP–bound forms can be examined by superposing subunit outlines for top, bottom, and side views (Figure 4). In Figure 4a, the three top views are superposed, showing the clockwise pivoting of apical domains about the hinge region (indicated by the asterisk) in the sequence GroEL (shaded)–GroEL-ADP–GroEL-ATP. This would cause the substrate-binding site (shown as a bar on one subunit) to be rotated out of the central channel, towards the intersubunit interface. The bottom views (Figure 4b) show that the lower apical domains pivot anticlockwise in ADP (seen as clockwise when viewed from below, as in Figure 4b) but that the main movement in ATP is radially inward. This would have a similar effect in burying the substrate-binding sites. In Figure 4c, the side views show the pronounced twisting out of the apical domains in the GroEL-ADP structure relative to GroEL (shaded); the whole oligomer is more open and expanded. In GroEL-ATP (Figure 4d), there is a further slight twisting and closing of subunits relative to GroEL-ADP (light shading); the subunits in the lower ring are rotated inwards, giving a more asymmetric (loss of 2-fold) structure.

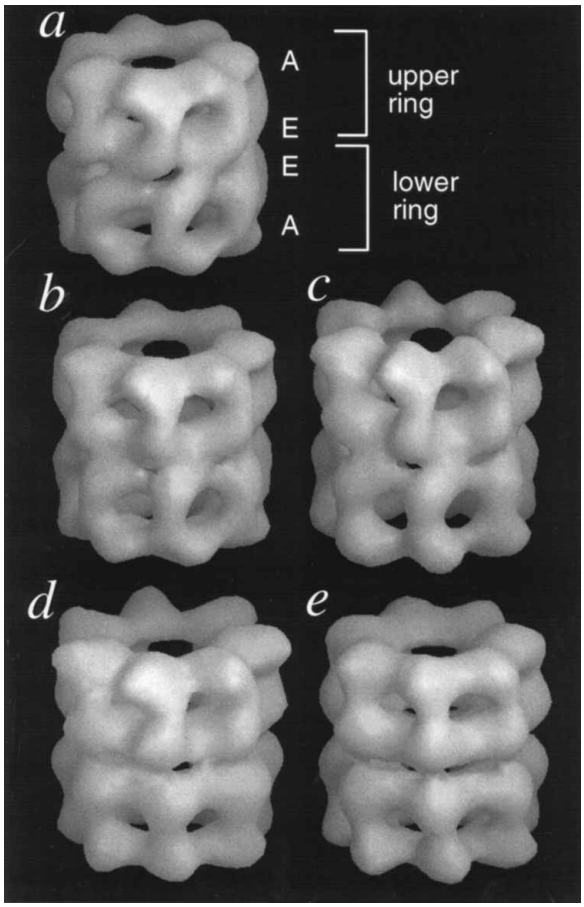

Figure 3. 3-D Reconstructions of GroEL–Nucleotide Complexes

(a) GroEL crystal structure (Braig et al., 1995) converted to electron density and filtered to 30 Å resolution, shown by surface rendering. A, apical domains; E, equatorial domains.
Cryo-EM 3-D reconstructions of GroEL–nucleotide complexes:
(b) GroEL 3-D reconstruction;
(c) GroEL-ADP;
(d) GroEL-AMP-PNP;
(e) GroEL-ATP. Each of the nucleotide structures is different; they are all more extended than GroEL, with the upper apical domains twisted out. The contour level for each structure was chosen to enclose the correct molecular volume in this and all other figures, as explained in Experimental Procedures. Each EM data set contained about 1000 images.

The domain movements in the GroEL ATPase cycle are best appreciated by viewing the succession of forms as a movie, available as additional material on the Web site http://www.cell.com.

Significance Tests for the Structural Changes

In order to quantitate structural changes occurring during the ATPase cycle, we compared the GroEL, GroEL-ADP, and GroEL-ATP structures using the Student's t test. In Figures 5a and 5b, the GroEL-ADP structure is shown colored according to the significance level of its differences with unliganded GroEL (Figure 5a) and with GroEL-ATP (Figure 5b). Each comparison is shown whole and partly cut open to allow a view into the inside of the cage. Blue regions indicate that no significant

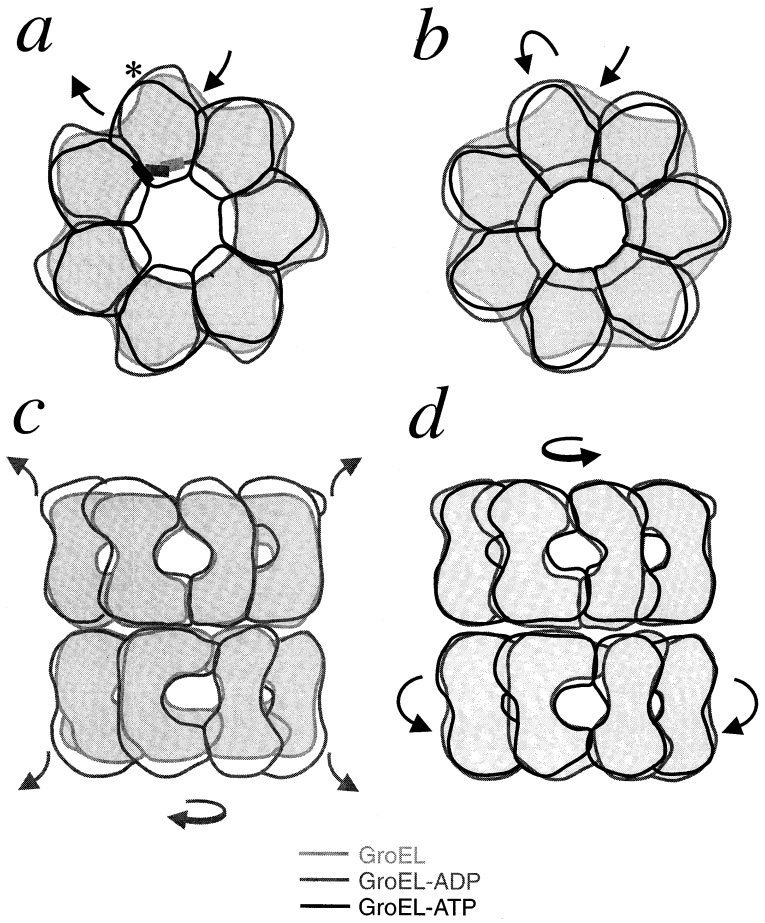

Figure 4. Domain Movements in GroEL Subunits Induced by ADP and ATP Binding

Overlays of subunits for GroEL (light gray) and its ADP (medium gray) and ATP–bound (black) forms. The three structures were aligned using the relatively fixed regions around the equatorial domains.

(a) Top view showing the progressive clockwise twist of apical domains about hinge 2 (whose approximate location is shown by the asterisk), from GroEL (shaded)→ADP→ATP. The shaded bars indicate the way in which the domain twisting would move the substrate-binding site from its position in GroEL facing the central channel, towards occlusion in the intersubunit interface in GroEL-ATP.

(b) Bottom view, showing the same sequence as in (a) for the lower ring. The lower GroEL cavity is more closed. ADP causes an anticlockwise twist (clockwise when seen from below), but ATP mainly causes a radially inward movement.

(c) Side view of GroEL (shaded) and GroEL-ADP, showing the pronounced vertical expansion of the oligomer.

(d) Side views of GroEL-ADP and GroEL-ATP. The ATP subunits in the upper ring twist slightly, whereas those in the lower ring rock inwards. The cavity diameter is smaller in ATP than in ADP.

change is detected, whereas red coloring indicates differences significant at $p << 0.0005$ (p, probability that the differences are due to chance). The comparison between GroEL-ADP and GroEL (Figure 5a) highlights the ends of the apical domains, which are rotated away from the equatorial domains, and a localized region of change around hinge 1. However, the central part of the structure, in the region of the interring contacts, does not show signficant differences. In contrast, the comparison between GroEL-ADP and GroEL-ATP structures (Figures 5b and 5c) reveals a highly significant region of change around one of the interring contacts (red areas at the front center of the structure in Figures 5b and 5c, left). In Figure 5c, the GroEL-ATP structure is shown, colored according to the significance of differences between it and the GroEL-ADP structure. The comparison between ADP and ATP structures shows that they have different degrees of twist in the apical domains, that the lower cavity is more closed in ATP, and that there is a localized region of difference around the interring contact between the "windows" (the large holes between neighboring subunits within each ring; contact 1 in Figure 1). There is also a small region of significant difference adjacent to interring contact 2 (Figure 5c).

Nucleotide-Induced Changes in GroEL–GroES Complexes

The full chaperonin system involves complexes between GroEL and GroES. In the presence of adenine nucleotides, GroEL has very high affinity for one GroES and low affinity for a second GroES (Chandrasekhar et al., 1986; Bochkareva et al., 1992; Todd et al., 1994; Llorca et al., 1994). These complexes show much greater rotations and distortions of the apical domains in the cis (GroES-bound) ring of GroEL (Figure 6). Thin bridges of density at the sites of contact between GroEL and GroES are the correct size and position to contain the mobile loop regions of GroES in an extended conformation (Landry et al., 1993; Hunt et al., 1996). The central hole in the GroES is also resolved in these maps. Football structures (Figure 6d) were separated from bullet structures (Figures 6b and 6c) by cross-correlation, testing each image against reference projections from both types of structure. Footballs accounted for 15%–30% of the side views with ATP in the steady state (after 10–20 min in 2.5 mM ATP) and 60%–70% of the side views with AMP-PNP (5 mM). It has been previously reported that footballs are not seen with 2 mM ATPγS (Llorca et al., 1994). The handedness of the football reconstruction was chosen arbitrarily to match the upper ring of the AMP-PNP bullet.

The GroEL–GroES bullet complexes in ADP, AMP-PNP, and ATP show a more restricted range of movements than the corresponding GroEL–nucleotide complexes. Among the bullet structures, the apical domains are in slightly different positions. In the ADP bullet (Figure 6a), the trans apical domains are more twisted out radially than in AMP-PNP or ATP, and the cis apical

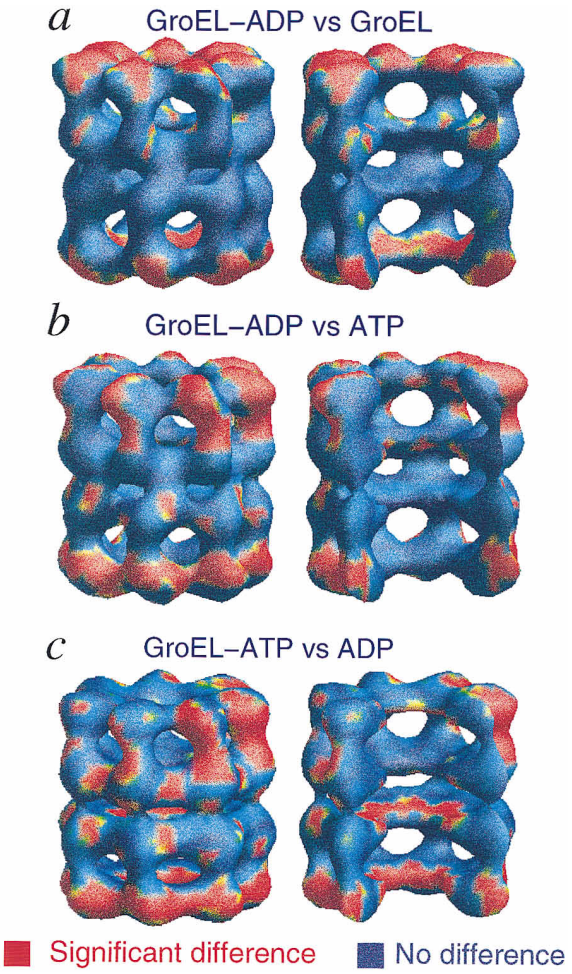

Figure 5. Significance Maps of Differences between GroEL and Its ADP and ATP Complexes

A quantitative comparison of the structures in ADP, ATP, and without nucleotide is shown by coloring the surfaces according to the significance level from t tests between the data sets. Blue regions show no significant changes, and red regions indicate differences significant at $p << 0.0005$.

(a) GroEL-ADP, whole and partially cut open to show internal features, colored according to the significance map of its comparison with GroEL. The differences are confined to the apical domains and to a localized region around hinge 1.

(b) GroEL-ADP, colored according to the t test comparison with GroEL-ATP. This comparison shows further twisting of the apical domains, rocking of the lower equatorial domains, and a significant difference in a small region in the set of interring contacts between the windows (red patch on the center front of the structure).

(c) Similar representation of GroEL-ATP, showing the different rotations of the apical domains. Note the inward movement of binding site regions in the lower ring. The interring contact between the windows is very weak and appears absent at this contour level. Its position is flanked by vertical red streaks indicating highly significant differences.

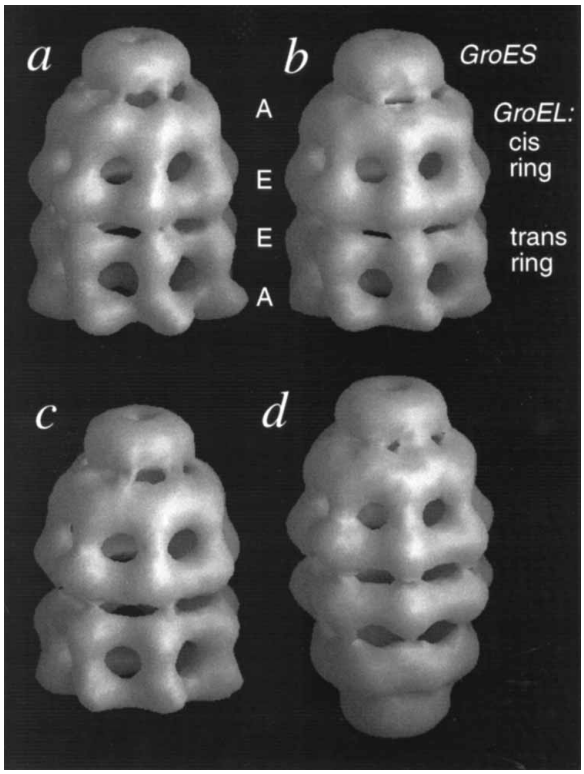

Figure 6. 3-D Reconstructions of GroEL–GroES Complexes

3-D reconstructions of (a) GroEL–GroES-ADP, (b) GroEL–GroES-AMP-PNP, (c) GroEL–GroES-ATP, and (d) GroES–GroEL–GroES-AMP-PNP. The GroES-bound ring of GroEL adopts a completely different structure, with reversed handedness of subunit twist. A, apical domains; E, equatorial domains. The GroES and GroEL rings are labeled on (b).

domains have a slightly different tilt. In Figures 7a–7c, outlines of the ADP and ATP bullet structures are overlaid in side, top, and bottom views, showing the differences in twist between the subunits in the two forms. GroES is shaded. The slight twist of the cis apical domains (Figures 7a and 7b) rotates the contacts with GroES, shown as bars in Figure 7b. Overall, the complex is slightly more expanded in the ADP form, with the largest movement in the trans apical domains (Figure 7c). The pattern of conformational change is similar to that seen in GroEL–nucleotide complexes without GroES (Figures 3c and 3d), despite the large distortion of the cis apical domains.

Student's t tests between the bullet structures revealed highly significant differences (Figures 7d and 7e). The ADP complex is shown, whole and cut in half, colored according to the significance map of its differences with the ATP complex. The regions of significant change (red) are concentrated around the ends of the GroEL apical domains, the hinge regions at either end of the intermediate domains, the ends of the equatorial domains, and in GroEL interring contact 2 (Glu-461/Arg-452). There is a twist of the GroES subunits to accommodate the movement of the cis apical domains and rocking movements of the equatorial domains between the two states. The AMP-PNP bullet complex resembles the ATP complex.

The movements are best seen as movies showing alternating views of the two forms (http://www.cell.com).

Discussion

Mechanism of Allosteric Switching

The changes in GroEL interring contacts suggest a hypothesis for transmission of allosteric movements from

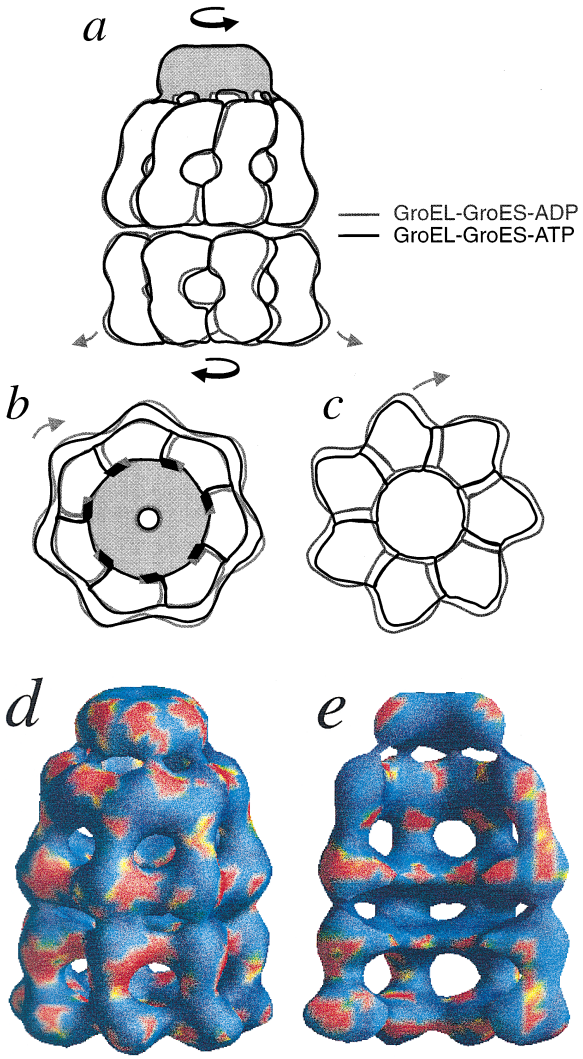

Figure 7. Domain Movements between GroEL–GroES-ADP and GroEL–GroES-ATP Complexes and Significance Maps of Their Differences

GroEL–GroES-ADP (gray outlines) and GroEL–GroES-ATP (black outlines) structures, viewed from the side (a), from above (b), and from below (c), showing the small twists of the subunit domains. GroES is shaded. The top view in (b) shows the outlines of the cis apical and equatorial domains surrounding the GroES. The bottom view in (c) shows only the trans apical domains.

(d and e) Student's t test comparison of these structures, color-coded by the significance map of their differences, as in Figure 5. The main regions of difference in GroEL (red) are the ends of the apical domains, the ends of the equatorial domains, and the hinge regions. There is a localized region of significant variation at interring contact 2 (between the equatorial masses, on the outside surface of the structure). The pinwheel pattern of variation in GroES suggests that its subunits are being twisted by the change in GroEL apical domain orientation.

the nucleotide binding site. Regions around the two contact sites in the GroEL crystal structure (Braig et al., 1995) are overlaid on the EM reconstructions in ADP and ATP, respectively, in Figures 8a and 8b. The EM reconstructions are shown as white wire-frame surfaces, and the charged residues in the contacts are shown in blue and red (positive and negative residues, respectively). The helix (green) connecting Lys-105 in contact 1 to nucleotide phosphate–binding residues 87–91 and the ATP (purple) are also shown (Boisvert et al., 1996). The alignment was based on the close match between the GroEL crystal structure (Figure 3a) and EM reconstruction (Figure 3b) and the presence of relatively fixed reference points (intermediate domains) in all the structures. Contact 1, involving residues Lys-105 and Glu-434, shown to be a site of significant variation between the structures by the t test, is shown at the front center of the structures. The connecting density in the ADP structure is greatly reduced and seen as a hole in the front of the ATP structure. The hole to the left of that contact is not resolved in the GroEL and GroEL-ADP structures, but the t test results suggest that there is no significant change occurring in that position. At the resolution of this study, the two contacts are not separated, but their locations, between the windows and between the equatorial domains for contacts 1 and 2, respectively, are unmistakable. (The centers of mass of structural features and difference densities can be determined to much higher accuracy than the spatial resolution, which is a measure of the center-to-center distance between the closest objects that can be resolved into separate peaks of density).

We propose that ATP turnover causes allosteric switching between the rings by altering the interring contact about Glu-434/Lys-105. Small displacements of the helix linking Thr-91, in the ATP binding site, to Lys-105, in the contact, might be sufficient to weaken the interaction by withdrawing the lysine, altering the balance of charges in the contact. There is some indication of change around the other contact (Glu-461/Arg-452) in GroEL complexes, and definite changes are seen in this region in GroEL–GroES complexes. Since mutation of Glu-461 interferes with GroES binding and blocks polypeptide release (Fenton et al., 1994), this points to an important ATP/ADP allosteric change relating contact 2 and the GroES/substrate-binding sites. Changes in both contacts may cause or result from rocking movements of the equatorial domains.

Nucleotides Open the GroEL Cage and Occlude the Substrate-Binding Regions

The movements of the apical domains of GroEL in the different states are shown by superposing approximate outlines for the domains in Figures 9a and 9b. All the nucleotide forms show a vertical expansion (perhaps by opening of the equatorial–intermediate hinge; hinge 1 on Figure 1), and there is a progressive twisting of the apical domain around the axis (rotation of the intermediate–apical hinge; hinge 2) in the sequence ADP, AMP-PNP, and ATP for the upper ring. (In the lower ring, the sequence is slightly different, since the AMP-PNP structure is ADP–like in the upper ring and ATP–like in the lower ring.) In Figure 9a, the progressive twisting is shown for two adjacent apical domains from GroEL to ADP to ATP. Figure 9b shows the outline of one subunit in the cis ring of the GroEL–GroES-ATP complex compared with the same subunit in GroEL and in GroEL-ATP, also revealing a progressive rotation and vertical extension of the apical domain. On the basis of this 30 Å resolution data, the movements of the GroEL apical domains appear to follow the arc of the hinge rotation.

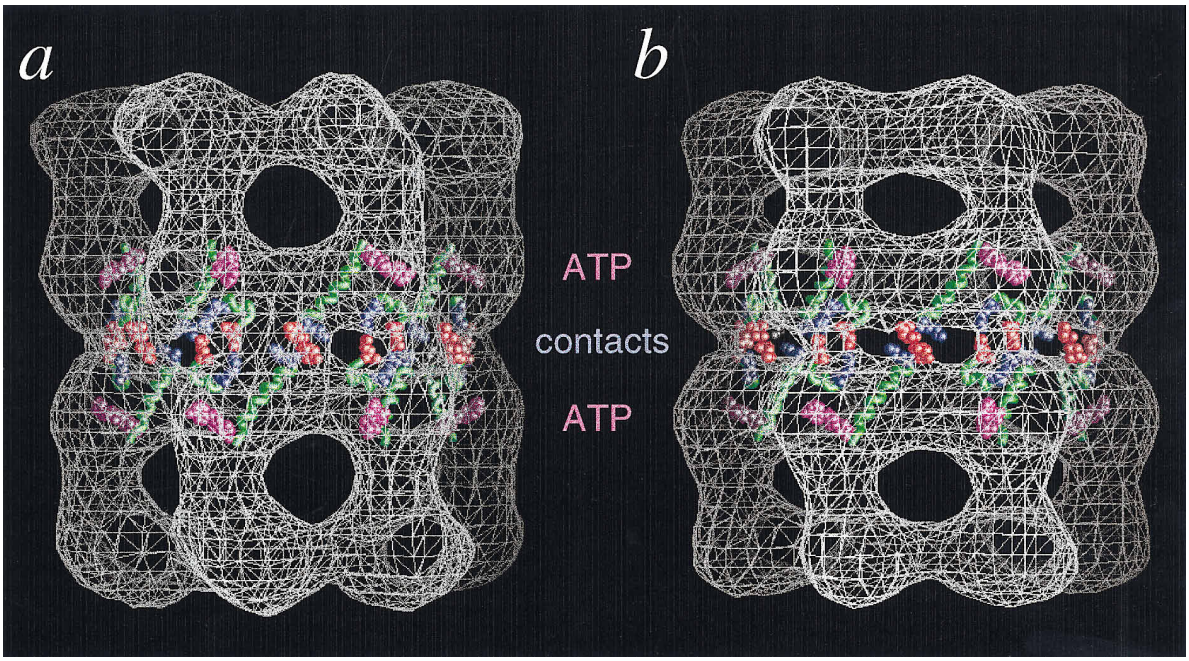

Figure 8. GroEL–ADP and GroEL–ATP Reconstructions Aligned with the Atomic Structure of the Interring Contacts and Their Connection to the ATP Binding Site

GroEL-ADP (a) and GroEL-ATP (b), aligned with the atomic structure of the interring contact regions of GroEL. The EM reconstructions are shown as wire frame surfaces (white) to reveal the atomic models inside. Interring contact 1 is at the front center of each structure and is seen as solid density in the ADP reconstruction and as a hole in the ATP reconstruction. The positively and negatively charged residues in the contacts are shown in blue and red, respectively. The helix (green) connecting the central contact (Lys-105) to the ATP binding site (Thr-91) extends diagonally outward from the contact, with an ATP molecule (purple) bound in each site.

One component of this motion is a twist around a vertical axis, and the other is a rotation in the vertical plane. There is probably also a component of vertical opening from hinge 1.

The most open form of GroEL is found in the presence of ADP. In this case, both rings have had a (mainly axial) hinge opening, making the oligomer taller. This explains the biochemical finding that ADP decreases the stability of GroEL, implying a more open structure (Gorovits and Horowitz, 1995).

The twisting motion is likely to rotate the substrate-binding sites, which face the central channel in GroEL (Fenton et al., 1994) away from the central cavity and towards the subunit contact regions (Figures 4a and 9a). This would have the effect of progressively occluding the binding sites and is in excellent agreement with the progressive reduction of binding affinity of GroEL for nonnative lactate dehydrogenase in the same series of nucleotide complexes (Staniforth et al., 1994).

Movements in GroEL–GroES Complexes: Implications for Encapsulated Folding Substrates

In the complexes with GroES, binding of GroES is accompanied by a major rotation and change in twist of the apical domains, a continuation of the motion induced by ATP binding to GroEL alone (Figure 9b). The cis apical domains of GroEL radically change shape, and the twist of the subunits reverses handedness on binding GroES. Because of this large distortion, the surface exposed for potential substrate interactions may be very different from that in unliganded GroEL. A further site of allosteric movement for GroES-bound complexes is in the Glu-461/Arg-452 contact. Despite these differences, the relative displacements in ADP and ATP bullet complexes are similar to those observed in the absence of GroES.

The presence of distinct cis apical domain conformations depending on nucleotide is consistent with an ATP–induced change in interaction with a substrate trapped under GroES, as implied by the observed changes in fluorescence anisotropy of trapped substrates (Weissman et al., 1996). Switching between these different states is likely to be important in the assisted folding mechanism. A molecular interpretation of the movements of substrate-binding sites in the GroES complexes is not yet possible and will have to await the atomic structure determination of at least one of the GroEL–GroES complexes. Movements of the apical domains while they are bound to GroES causes twisting in GroES, which has been suggested to be a metastable structure by Hunt et al. (1996), as well as rotation of the mobile loop contacts (Figure 7). The significance map indicates global changes in GroEL–GroES complexes during the ATPase cycle (Figures 7d and 7e), in accord with the mutagenesis findings of Fenton et al. (1994).

Comparison with the Crystal Structure of GroEL–ATPγS

In the presence of the nonhydrolyzable analog AMP-PNP, the structure adopts a conformation intermediate between those of GroEL-ADP and GroEL-ATP. There

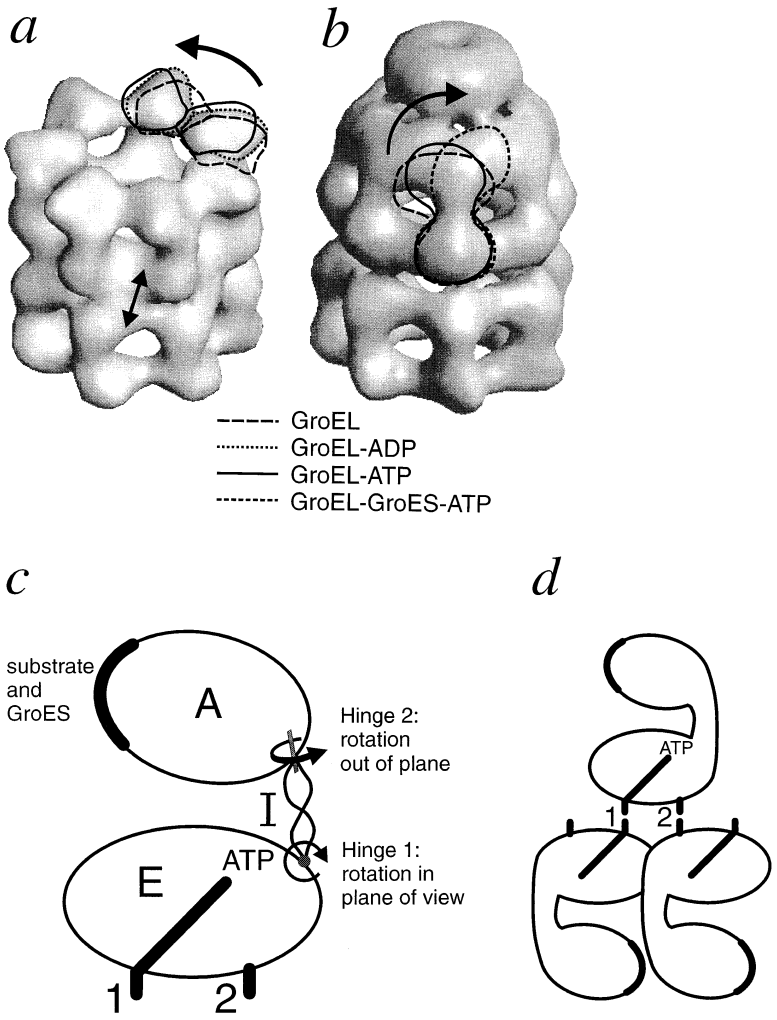

Figure 9. Apical Domain Movements, Hinge Rotations, and Interring Communication in the GroEL Functional Cycle

(a) Diagram showing the displacement of two adjacent apical domains in GroEL, GroEL-ADP, and GroEL-ATP, outlined on the GroEL-ADP structure. The apical domains pivot about hinge 2 (Figure 1). Changes around the 434/105 interring contact are indicated by the double-headed arrow. The swiveling of the apical domains rotates the substrate-binding sites away from their original position facing the central cavity and towards the intersubunit interface.

(b) Outline of one GroEL subunit in GroEL, GroEL-ATP, and GroEL–GroES-ATP, superposed on the complex with GroES. The apical domain goes through a progressive twist and upward movement. The handedness for all structures was chosen to match the lower (less opened) ring to the GroEL crystal structure.

(c) Schematic model of allosteric transmission from nucleotide binding to changes in hinge rotation and interring contacts. The effect of nucleotide on the binding pocket extends to the interring contacts via the linker helix (diagonal line) and controls hinge rotations by affecting hinge 1, either directly or by modulating the interring contacts, and thereby rocking the equatorial domain. This is postulated to transmit via concerted motion in the intermediate domain to twist the apical domain out of the plane, around hinge 2, thus controlling the position and accessibility of the substrate-binding sites. A, apical; E, equatorial; I intermediate domains; 1, 2, interring contacts.

(d) A subunit in the upper ring makes contacts with two subunits in the lower ring. The postulated route for transmission of cooperative effects is shown through the linker helices and contact 1, represented as in (c).

remains a discrepancy between these cryo-EM results and the crystallographic results on GroEL-ATPγS complexes (Boisvert et al., 1996). In that study, the nucleotide binding site was revealed, but the changes seen in the structure were extremely small and did not make apparent a mechanism for progagating the changes in the nucleotide binding pocket to the base of the equatorial domain and to the hinge rotating the apical domain. The reasons for this apparent discrepancy with the EM work are unclear. The crystallographic work was done on the double mutant R13G/A126V, which has reduced negative cooperativity (Aharoni and Horovitz, 1996), and with ATPγS, which may have different effects on GroEL than AMP-PNP. Finally, the great variety of conformations detected in this study suggest that the GroEL subunits are extremely flexible. Packing of such a flexible structure in the crystal lattice may reverse the hinge rotation observed by cryo-EM on complexes in solution.

Relation between Structural and Allosteric States

The cooperative mechanism of GroEL ATPase has been analyzed in terms of T (tense) and R (relaxed) states, according to the Monod–Wyman–Changeux theory, extended to take into account the positive cooperativity within rings and negative cooperativity between rings (Yifrach and Horovitz, 1994, 1995, 1996; Kovalenko et al., 1994). Unliganded GroEL is mainly in the TT state, and ATP binding converts it to TR and at high ATP concentrations to RR. The R state favors GroES binding, so that RR states would be able to form footballs. The GroEL-ATP structure described here (in 2.5 mM ATP; Figure 3e) represents an ATP–bound state, since the same structure is observed at short times (within one round of ATP turnover) and in the steady state, and hydrolysis is the rate-limiting step (Jackson et al., 1993; Burston et al., 1995). Consistent with the structural asymmetry, our steady-state conditions have been found to produce a TR state (O. Yifrach and A. Horovitz, personal communication).

The ADP state is intermediate in character between T and R states, since it has less twist (Figures 4a and 9a) and only slowly binds GroES (Jackson et al., 1993). It has recently been assigned to an R-like but distinct allosteric state (O. Yifrach and A. Horovitz, personal communication).

Our analysis suggests that the R state is a collection of structural forms in which the GroEL apical domains are twisted about the intermediate–apical hinge region,

and the hinge region is flexible and able to undergo the large rotation required for GroES binding (Figures 9a and 9b). There is an obvious mechanical basis for the positive cooperativity within the heptameric rings: the twisting can only take place as a concerted motion; otherwise, untwisted domains would block the motion. The mechanism of negative cooperativity appears more complicated, since it involves rotations propagated through the whole GroEL subunit.

Further complexity is added by the GroES-bound states. GroES binding involves a very large conformational change; it increases the cooperativity of ATP hydrolysis (Gray and Fersht, 1991) and favors the R state (Kovalenko et al., 1994). Bullet complexes containing only ADP (Figure 6a) have high affinity for substrates and are usually inactive in folding. In the presence of ATP (Figure 6c), they have a different conformation and are active in folding (Mayhew et al., 1996; Weissman et al., 1996). It has also been suggested that football complexes improve the efficiency of folding (Azem et al., 1995).

Conclusions: Structural Basis for the Allosteric Mechanism of GroEL Action

This work reveals an extraordinary range of domain movements in GroEL. Allosteric R states are characterized by flexibility of the interdomain hinge region around glycines 192 and 375 (hinge 2, Figure 1). A schematic model for the mechanism (Figure 9c) is based mainly on rigid body rotations of the equatorial and apical domains, coupled by twisting or other concerted change through the intermediate domain. The long-range effects of mutations in the intermediate domain have led Fenton et al. (1994) to suggest that it transmits allosteric interactions. We propose that the nucleotide binding site exerts control on the allosteric state and substrate-binding properties by transmitting movements in two directions: first, nucleotide binding causes rotations around hinge 1, either directly or by modulating the interring contacts via movements of helix 92–104 (diagonal line in Figure 9c), leading to reorientation of the equatorial domain about hinge 1. Changes in the contacts are transmitted to the opposite ring via the equivalent helix in the lower subunit (Figure 9d), mediating negative cooperativity. Second, to explain the specific effects of different nucleotides on the twist of the apical domains, we propose that the changes in hinge 1 are propagated through the intermediate domain, inducing large rotations of hinge 2, thereby twisting the apical domains and controlling substrate and GroES binding.

Thus, changes in conformation are cooperatively propagated from the base of the GroEL equatorial domains right through to the tips of the apical domains in both rings, modulating the accessibility of the substrate-binding sites, in both the absence and presence of GroES. These conformational changes are likely to be fundamental to the mechanism by which the GroE system chaperones protein folding.

Experimental Procedures

Protein Preparation and Solutions

Escherichia coli GroE proteins were prepared as previously described (Burston et al., 1995; Fenton et al., 1994). Nucleotides were obtained from Boehringer. The GroEL concentration in the EM samples was 1 mg/ml, in 10 mM KCl, 10 mM Tris (pH 7.5), 8 mM $MgCl_2$. GroES was added in a 3-fold molar excess to GroEL. Complexes were incubated for 10–20 min with nucleotide (ADP, AMP-PNP, 5 mM; ATP, 2.5 mM) before vitrification. GroEL–ATP complexes were also vitrified within 4 s of ATP addition by mixing GroEL and ATP on the EM grid just before vitrification.

EM

Samples were vitrified on EM grids and imaged on a JEOL 1200 EX transmission EM at 120 kV with an Oxford Instruments cryotransfer stage, as previously described (Chen et al., 1994). Images were recorded on Agfa EM film with an electron dose of approximately 10 e/Å^2. The first zero of the contrast transfer function was beyond (22 Å)$^{-1}$ in all cases.

Image Processing

Film scanning and particle selection were done using Semper software (Synoptics Ltd.) on PCs, and subsequent alignment and 3-D reconstructions were done using Spider (Frank et al., 1996) on either Digital alpha or Silicon Graphics workstations. Films were scanned at a final sampling of 5.6 Å/pixel on a CCD camera. Molecules were interactively selected from scanned areas and cut out into 64 $\times$ 64 pixel boxes. All particles recognizable as chaperonin side views and not in contact with other structures were selected. The cut-out particles were band-pass filtered between 256–25 Å and then normalized to the same mean and standard deviation. No correction for the contrast transfer function was applied.

3-D Reconstruction

An angular refinement procedure (Penczek et al., 1994; Baker and Cheng, 1996; Schatz et al., 1995; Radermacher, 1994) was adapted for the chaperonin data, using Spider. Starting models were already available, created by assuming that all side views had the same orientation and back-projecting their average with the known 7-fold symmetry (Chen et al., 1994). That strategy gave models with very poor angular resolution. Reconstructions with better angular resolution could be made by first using correspondence analysis to classify the side views into different azimuthal orientations around the 7-fold axis. However, the latter procedure was found to be unnecessary, since either starting model led to the same final structure after several rounds of refinement.

Orientations of the molecules in the set of images were determined by cross-correlating each image with a set of reference projections made from the starting model and normalized to a common mean and standard deviation. A set of three parameters (x and y shifts and in-plane rotation) were refined in 2-D against each reference projection, and the set of reference projections represents a search of two orientation parameters in 3-D. Thus, this procedure was a simultaneous five-parameter search for each image. The image orientation was assigned according to the reference image giving the best correlation. A new model was generated, using the new alignment parameters for each image, and the procedure was iterated, starting with the same original images, until the models converged.

The chaperonin side views are all very nearly perpendicular to the 7-fold axis. This preferential orientation and the 7-fold symmetry reduce the number of views required in the 3-D orientation search. A sampling interval around the 7-fold axis of $3.2^\circ \left(\frac{360}{7 \times 16}\right)$, spanning one-seventh of a turn, was used. The first 16 views are perpendicular to the axis. For the next 16 views, azimuthal distribution is the same, but the 7-fold axis is tipped out of the plane by 6.4°, and a third set of 8 views spaced at 6.4° is tipped by 12.9°. Most images correlate best with the least tipped reference images and very few with the 12.9° images. The variance within each angular class was used to check that the classes were homogeneous. Towards the end of the refinement, 10%–30% of the images with the lowest correlation coefficients were excluded from some data sets. The 12.9° tipped images were not used.

Reconstructions were calculated using iterative back projection, as implemented in Spider. The resolution of each reconstruction was assessed by splitting the data set into two and calculating two

independent reconstructions, which were then compared by Fourier ring correlation and phase-residual methods. The more conservative phase residual was found to be more realistic. This was established by comparing the GroEL reconstruction with a map made from the atomic structure (Braig et al., 1995), low-pass filtered to a range of resolutions. The structures are viewed as rendered surfaces using AVS (Advanced Visualization System) software. The contour level for each structure was chosen so that the surface enclosed the correct molecular volume, assuming a protein density of 1.37 g/cm^3.

Reproducibility and Significance of Differences between Reconstructions

The refinement procedure was robust to changes in starting model, and structures always converged unless the raw data were of very poor quality. In comparisons of ADP– and ATP–bound structures, starting models were interchanged, but the refinements always reverted to the original structure within a few rounds of iteration. For the GroEL–nucleotide structures presented here, the final refinements were all started from a 25 Å resolution map of the crystal structure. To test the deviations from 2-fold symmetry, models were 2-fold averaged and refinements restarted. In all cases, the asymmetry returned with refinement.

To test the statistical significance of differences between the different nucleotide-bound forms, the data sets were each divided up to make four separate reconstructions, and the sets were compared with a Student's t test (Milligan and Flicker, 1987). For internal comparisons, data sets were divided up to make eight independent reconstructions. The internal comparisons did not show differences significant at $p << 0.025$ (p, probability that the differences are due to chance). The differences considered to be significant were at $p < 0.0005$. The positions of the connecting intermediate domains, and thus the locations of the windows in the oligomer, could be aligned in all the structures, providing a fixed region about which the other domains pivoted. The alignment was done manually, using AVS software, and could be optimized within 1°–2° rotations about the fixed 7-fold axis. Figure 8 was produced with GRASP (Nicholls et al., 1993), by reading in the 3-D recontructions in potential file format.

Acknowledgments

We thank Juliet Munn for excellent EM support. We are particularly grateful to Richard Westlake for enabling us to make use of all possible computing capacities for this work and to David Houldershaw for setting up software and writing conversion programs for different data formats. We also thank John Bouquiere, Ian Tickle, Judith Murray-Rust, and Gerald Tompsett for help with computing. We thank Tony Clarke, Steve Burston, Neil Ranson, Amnon Horovitz, Jonathan Weissman, Wayne Fenton, and Art Horwich for chaperonin proteins and many helpful discussions. We thank Ron Milligan for the t test programs, Richard Sessions for use of the computing facilities in the Bristol Biochemistry Department, and the Wellcome Trust and Biotechnology and Biological Sciences Research Council for funding. Some processing was done using the Supercomputing Resource in Molecular Biology at European Molecular Biology Laboratory (Heidelberg).

Received May 3, 1996; revised August 16, 1996.

References

Aharoni, A., and Horovitz, A. (1996). Inter-ring communication is disrupted in the GroEL mutant Arg13→Gly; Ala126→Val with known crystal structure. J. Mol. Biol. *258*, 732–735.

Azem, A., Diamant, S., Kessel, M., Weiss, C., and Goloubinoff, P. (1995). The protein folding activity of chaperonins correlates with the symmetric $GroEL_{14}(GroES_7)_2$ heterooligomer. Proc. Natl. Acad. Sci. USA *92*, 12021–12025.

Baker, T.S., and Cheng, R.H. (1996). A model-based approach for determining orientations of biological macromolecules imaged by cryoelectron microscopy. J. Struct. Biol. *116*, 120–130.

Bochkareva, E.S., and Girshovich, A.S. (1994). ATP induces nonidentity of two rings in chaperonin GroEL. J. Biol. Chem. *269*, 23869–23871.

Bochkareva, E.S., Lissin, N.M., Flynn, G.C., Rothman, J.E., and Girshovich, A.S. (1992). Positive cooperativity in the functioning of molecular chaperone GroEL. J. Biol. Chem. *267*, 6796–6800.

Boisvert, D.C., Wang, J., Otwinowski, Z., Horwich, A.L., and Sigler, P.B. (1996). The 2.4 Å crystal structure of the bacterial chaperonin GroEL complexed with ATPγS. Nature Struct. Biol. *3*, 170–177.

Braig, K., Otwinowski, Z., Hegde, R., Boisvert, D.C., Joachimiak, A., Horwich, A.L., and Sigler, P.B. (1994). The crystal structure of the bacterial chaperonin GroEL at 2.8 Å. Nature *371*, 578–586.

Braig, K., Adams, P.D., and Brunger, A.T. (1995). Conformational variability in the refined structure of the chaperonin GroEL at 2.8 Å resolution. Nature Struct. Biol. *2*, 1083–1094.

Burston, S.G., Ranson, N.A., and Clarke, A.R. (1995). The origins and consequences of asymmetry in the chaperonin reaction cycle. J. Mol. Biol. *249*, 138–152.

Chandrasekhar, G.N., Tilley, K., Woolford, C., Hendrix, R., and Georgopoulos, C. (1986). Purification and properties of the groES morphogenetic protein of *Escherichia coli*. J. Biol. Chem. *261*, 12414–12419.

Chen, S., Roseman, A.M., Hunter, A., Wood, S.P., Burston, S.G., Ranson, N., Clarke, A.R., and Saibil, H.R. (1994). Location of a folding protein and shape changes in GroEL–GroES complexes imaged by cryo-electron microscopy. Nature *371*, 261–264.

Fenton, W.A., Kashi, Y., Furtak, K., and Horwich, A.L. (1994). Residues in chaperonin GroEL required for polypeptide binding and release. Nature *371*, 614–619.

Frank, J., Radermacher, M., Penczek, P., Zhu, J., Li, Y., Ladjadj, M., and Leith, A. (1996). SPIDER and WEB: processing and visualization of images in 3-D electron microscopy and related fields. J. Struct. Biol. *116*, 190–199.

Goloubinoff, P., Christeller, J.T., Gatenby, A.A., and Lorimer, G.H. (1989). Reconstitution of active dimeric ribulose bisphosphate carboxylase from an unfolded state depends on two chaperonin proteins and Mg-ATP. Nature *342*, 884–889.

Gorovits, B.M., and Horowitz, P.M. (1995). The chaperonin GroEL is destabilized by binding of ADP. J. Biol. Chem. *270*, 28551–28556.

Gray, T.E., and Fersht, A.R. (1991). Cooperativity in ATP hydrolysis by GroEL is increased by GroES. FEBS Lett. *292*, 254–258.

Hartl, F.U. (1996). Molecular chaperones in cellular protein folding. Nature *381*, 571–580.

Hunt, J.F., Weaver, A.J., Landry, S., Gierasch, L., and Deisenhofer, J. (1996). The crystal structure of the GroES co-chaperonin at 2.8 Å resolution. Nature *379*, 37–45.

Jackson, G.S., Staniforth, R.A., Halsall, D.J., Atkinson, T., Holbrook, J.J., Clarke, A.R., and Burston, S.G. (1993). Binding and hydrolysis of nucleotides in the chaperonin catalytic cycle: implications for the mechanism of assisted protein folding. Biochemistry *32*, 2554–2563.

Kovalenko, O., Yifrach, O., and Horovitz, A. (1994). Residue lysine-34 in GroES modulates allosteric transitions in GroEL. Biochemistry *33*, 14974–14978.

Landry, S.J., Zeilstra-Ryalls, J., Fayet, O., Georgopoulos, C., and Gierasch, L.M. (1993). Characterization of a functionally important mobile domain of GroES. Nature *364*, 255–258.

Langer, T., Pfeifer, G., Martin, J., Baumeister, W., and Hartl, F.-U. (1992). Chaperonin-mediated protein folding: GroES binds to one end of the GroEL cylinder, which accommodates the protein substrate within its central cavity. EMBO J. *11*, 4757–4765.

Llorca, O., Marco, S., Carrascosa, J.L., and Valpuesta, J.M. (1994). The formation of symmetrical GroEL–GroES complexes in the presence of ATP. FEBS Lett. *345*, 181–186.

Martin, J., Langer, T., Boteva, R., Schramel, A., Horwich, A., and Hartl, F.-U. (1991). Chaperonin-mediated protein folding at the surface of groEL through a "molten globule"-like intermediate. Nature *352*, 36–42.

Martin, J., Mayhew, M., Langer, T., and Hartl, F.U. (1993). The reaction cycle of GroEL and GroES in chaperonin-assisted protein folding. Nature *366*, 228–233.

Mayhew, M., da Silva, A.C.R., Martin, J., Erdjument-Bromage, H., Tempst, P., and Hartl, F.U. (1996). Protein folding in the central cavity of the GroEL–GroES chaperonin complex. Nature *379*, 420–426.

Milligan, R.A., and Flicker, P.F. (1987). Structural relationships of actin, myosin and tropomyosin revealed by cryo-electron microscopy. J. Cell Biol. *105*, 29–39.

Nicholls, A., Bharadwaj, R., and Honig, B. (1993). GRASP: graphical representation and analysis of surface properties. Biophys. J. *64* (2P12), A166.

Penczek, P., Grassucci, R.A., and Frank, J. (1994). The ribosome at improved resolution: new techniques for merging and orientation refinement in 3-D cryo-electron microscopy of biological particles. Ultramicroscopy *53*, 251–270.

Radermacher, M. (1994). Three-dimensional reconstruction from random projections: orientational alignment via radon transforms. Ultramicroscopy *53*, 121–136.

Saibil, H.R., Zheng, D., Roseman, A.M., Hunter, A.S., Watson, G.M.F., Chen, S., auf der Mauer, A., O' Hara, B.P., Wood, S.P., Mann, N.H., Barnett, L.K., and Ellis, R.J. (1993). ATP induces large quaternary rearrangements in a cage-like chaperonin structure. Curr. Biol. *3*, 265–273.

Schatz, M., Orlova, E., Dube, P., Jager, J., and van Heel, M. (1995). Structure of Lumbricus terrestris hemoglobin at 30 Å resolution determined using angular reconstitution. J. Struct. Biol. *114*, 28–40.

Staniforth, R., Burston, S.G., Atkinson, T., and Clarke, A.R. (1994). Affinity of chaperonin 60 for a protein substrate and its modulation by nucleotides and chaperonin 10. Biochem. J. *300*, 651–658.

Todd, M.J., Viitanen, P.V., and Lorimer, G.H. (1993). Hydrolysis of adenosine 5′ triphosphate by Escherichia coli GroEL: effects of GroES and potassium ion. Biochemistry *32*, 8560–8567.

Todd, M.J., Viitanen, P.V., and Lorimer, G.H. (1994). Dynamics of the chaperonin ATPase cycle: implications for facilitated protein folding. Science *265*, 659–666.

Weissman, J.S., Kashi, Y., Fenton, W.A., and Horwich, A.L. (1994). GroEL-mediated protein folding proceeds by multiple rounds of binding and release of nonnative forms. Cell *78*, 693–702.

Weissman, J.S., Hohl, C.M., Kovalenko, O., Kashi, Y., Chen, S., Braig, K., Saibil, H.R., Fenton, W.A., and Horwich, A.L. (1995). Mechanism of GroEL action: productive release of polypeptide from a sequestered position under GroES. Cell *83*, 577–587.

Weissman, J.S., Rye, H.S., Fenton, W.A., Beechem, J.M., and Horwich, A.L. (1996). Characterization of the active intermediate of a GroEL–GroES-mediated protein folding reaction. Cell *84*, 481–490.

Yifrach, O., and Horovitz, A. (1994). Two lines of allosteric communication in the oligomeric chaperonin GroEL are revealed by the single mutation Arg196→Ala. J. Mol. Biol. *243*, 397–401.

Yifrach, O., and Horovitz, A. (1995). Nested cooperativity in the ATPase activity of the oligomeric chaperonin GroEL. Biochemistry *34*, 5303–5308.

Yifrach, O., and Horovitz, A. (1996). Allosteric control by ATP of non-folded protein binding to GroEL. J. Mol. Biol. *255*, 356–361.